Sharp Carbon-Nanotube Tips and Carbon-Nanotube Soldering Irons

By *Abha Misra* and *Chiara Daraio**

High energy electron beam machining has been proven a powerful tool to modify desired nanostructures for technological applications[1–4] and to form molecular junctions and interconnections between carbon nanotubes.[2,5] A recent study[5] has shown the high degree of complexity in the creation of direct interconnections between multiwalled carbon nanotubes (MWCNTs) that have dissimilar diameters. We report on the nanoelectron-beam-assisted fabrication of atomically sharp iron-based tips and on the creation of a nanosoldering iron for nanointerconnects using Fe-filled MWCNTs. Our technique allows for carving a MWCNT into a nanosoldering iron, which was demonstrated as being capable of joining two separated halves of a tube. This approach could easily be extended to the interconnection of two largely dissimilar CNTs, a CNT and a nanowire, or two nanowires.

The development of the next generation of miniaturized electronic systems demands the integration of nanoelectronic components to create reliable mechanical and electrical contacts. Despite many years of CNT research, the electrical interconnection of individual nanotubes and nanowires remains a tedious task. At the same time, the development of scanning probe techniques and magnetic recording media require an ever decreasing tip size of ultrasharp magnetic read-write heads.[6] Recently, focused electron beams have been reported for the machining of both single-walled carbon nanotubes (SWCNTs) and MWCNTs, for cutting them, or for forming junctions at the atomic level (the latter being limited so far to only small and similar diameter tubes).[5] Along with the well known electrical, mechanical, and thermal properties of the CNTs, the presence of a metal filling inside their core has been suggested to enhance their applicability in magnetic recording media and new electronic devices, and to reinforce the material durability.[7,8] Here we report two interesting phenomena of nano-electron beam assisted machining of iron-filled MWCNTs: the fabrication of atomically sharp Fe-based tips and the direct interconnection of two large diameter MWCNTs. Previous attempts to solder CNTs had been performed through metal[5] and amorphous carbon[2] deposition at the tips, but the results showed little or questionable success.

The Fe-encapsulated CNTs considered for this study were produced by dissolution of a catalyst source (ferrocene) and a carbon source (toluene) in a thermal chemical vapor deposition system as described in the experimental section. Electron irradiation for manipulation, etching, and imaging was obtained in a transmission electron microscope (FEI Technai F-30 UT) with a field emission gun operating at an acceleration voltage (300 kV) without heating stage.

We first describe the creation of atomically sharp Fe-based tips (a schematic diagram of the process and the resultant structures is reported in Fig. 1a–d and the synthesis and operation of a CNT-soldering iron in Fig. 1e–f). It is shown that under controlled irradiation with a highly focused electron beam, Fe-filled MWCNTs can be cut at selected locations, similar to what was previously reported for MWCNTs[9] and for bundles of SWCNTs.[10] A MWCNT is sliced in two (Fig. 1b) and the Fe nanorods encapsulated inside the core of the tube are exposed to a continuous e-beam, centered in close proximity of the cut. This high energy irradiation causes an increase of the tube's internal pressure and to surface reconstruction at the incised rim. Transmission electron microscopy (TEM) observations of the described steps for the synthesis of an atomically sharp Fe-based tip are shown in Figure 2. The MWCNT studied had inner and outer diameters of 9 and 32 nm, respectively (Fig. 2a). Electron beam cutting was achieved by translating the CNT sample across its diameter under a nano e-beam (spot size 8 nm in diameter) with a current density of 1.3×10^3 A cm^{-2}. Figure 2b shows the process of formation of the opening in the MWCNT along the focused e-beam path. After a few seconds of cutting, the surface reconstruction at the unstable open ends of the carbon nanotube walls as well as on the surface of the Fe-nanorod is evident, as shown in Figure 2b and 2c (highlighted by the arrow). It is clear that because of a strong tendency towards the reduction of the surface energy,[11] the capping of the open wall ends occurs with the formation of a stable closed structure by cross linking between adjacent graphene planes (inter-wall interactions). This phenomenon results in the formation of semi-fullerene-like caps that interlink the walls and heal the incised surface. As a result the Fe nanorod near the incision remains trapped between the graphene caps on one side and the CNT's walls on the other. The self compression and dynamic behavior of encapsulated material inside graphitic networks, such as a carbon onion or MWCNTs, have been the subject of recent investigations.[12,13] It has been shown that under electron beam irradiation, high internal pressure and temperature caused local phase modification and shape changes of the metallic particles trapped inside the core.

[*] Prof. C. Daraio, Dr. A. Misra
Graduate Aeronautical Laboratories (GALCIT)
California Institute of Technology
Pasadena, CA, 91125 (USA)
E-mail: daraio@caltech.edu
Prof. C. Daraio
Applied Physics
California Institute of Technology,
Pasadena, CA, 91125 (USA)

DOI: 10.1002/adma.200801893

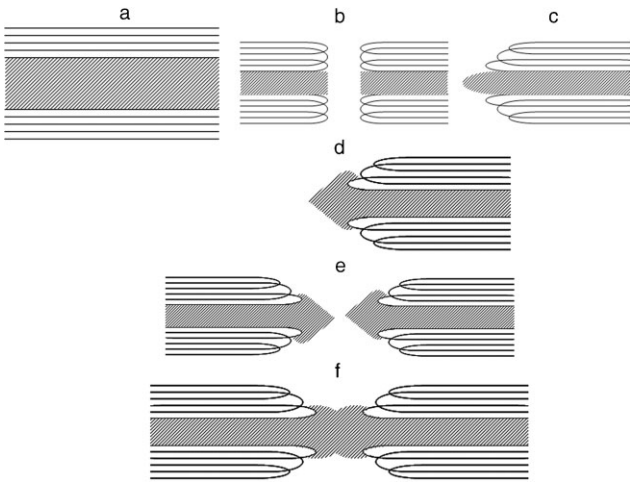

Figure 1. Processing steps for the formation of an atomically sharp Fe tip and of the soldering between two CNT halves under electron beam irradiation. a) As-grown Fe-encapsulated MWCNT. b) Electron-beam assisted cutting of a gap. c,d) Formation of the metal tip. e,f) Outward flow of the metal and final soldering of the CNT halves.

Upon continuous electron irradiation, the damage and reconstruction of the outermost carbon lattice further increased the pressure within the graphene cells, which enhanced such effects. Similarly, in our experiments it is evident that immediately after the reconstruction of the sliced walls' edges into a closed cell structure (Fig. 2c), the CNT starts behaving as a high pressure cell[12] for the encapsulated Fe nanorod. Because of the high pressure generation, Fe is pushed out from the nanotube's core and local restructuring phenomena occur. At the same time, the incised nanotube's edge begins to assume a pointed pencil-like shape. This phenomenon, similar to the one observed by Banhart et al.,[14] could be related to the generation and migration of vacancy/interstitial pairs in the inner walls, which caused the shrinking of the outer edges.

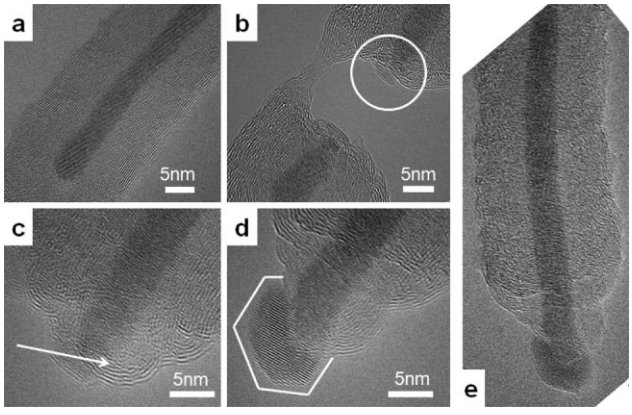

Figure 2. TEM snapshots showing the formation of an atomically sharp tip. a) TEM image showing the pristine CNT with an Fe (catalyst) nanorod encapsulated in its inner core. b) Cutting of a 10 nm gap across the tube (the area marked by a white circle underlines the edge of the Fe nanorod). c) High magnification image of the MWCNT wall's reconstruction into closed fullerene-like caps (marked by the arrow). d) Complete formation of the sharp Fe-tip after 17 min. e) Overall view of the MWCNT-supported sharp tip.

To further investigate the effects of electron irradiation, we studied the time evolution of the encapsulated Fe nanorod structure during the beam exposure of one side of the cut (upper edge of Fig. 2b). The Fe nanorod protrusion and the tip formation are shown in Figure 2c–d after ~17 min of e-beam irradiation. In addition to the outward extrusion of the nanorod towards the pressure gradient, the e-beam interaction also induces structure rearrangement on the exposed metal surface. Recently, the phenomenon of liquid-state surface faceting as a precursor to surface-induced crystallization was observed in a metal–alloy system under heating and irradiation.[4] In our system, no sample heating was provided and no liquidation of Fe crystals was observed in the TEM analysis. This suggests a different operative mechanism for the restructuring of the exposed Fe surface. The evolution in morphology may be attributed to quasi-melting,[15] where the restructuring is the result of fluid like behavior of atoms, which move to reach a thermodynamically favored configuration. This enables the formation of an atomically sharp tip (Fig. 2d) whose outer diameter is ~7 nm, and that has a vertex size of <1 nm. The complete formation of the restructured probe after ~17 min of e-beam irradiation is shown in Figure 2e. Because of the absence of a heating stage in our system, we could not preserve the initial parallel walls–tube structure, as the low defect mobility at room temperature prevents reconstruction and leads to rapid destruction of the graphite lattice. To ensure the graphite lattice reconstruction the specimen should be maintained at a temperature of >300 °C.[16]

The sharp tip suggests the possibility of utilizing the same structures for nano-soldering and interconnects, simply by prolonging the e-beam exposure of the tips to enable additional ejection of the metal tip. Such tips could then be used as nanosoldering irons if placed in proximity of one or two other elements to be connected. To explore the effective soldering ability of such probes, we performed a systematic investigation on various Fe-filled MWCNTs of different inner and outer diameters (20 and 60 nm) by using the same conditions of electron irradiation. Similar processing steps were followed for the cutting (Fig. 3a) and etching (Fig. 3b and 3c) of the tubes, with variable exposure time, dependent on the different tubes' diameters. It was demonstrated that the prolonged local electron irradiation on both sides of the incision causes an outward movement of the Fe nanorods that 'grow' towards each other until their successful final soldering. The TEM image reported in Figure 3c shows a complete merging and 'healing' of two previously separated halves of the CNT after ~30 min of e-beam exposure. From these results it is clear that the time needed for cutting and soldering of different nanotubes and/or nanowires depends on the outer diameter and number of walls composing the nanotubes. A higher magnification image of the soldered zone is shown in Figure 3d. The aggregation and restructuring of Fe at the junction is noticeable, and it is evident that surface modification phenomena took place all over the nanowire's area exposed to the e-beam. Remarkably, two distinct features were observed in the soldering process between the two Fe nanowires: the outward flow of the metal because of the pressure gradient created by the e-beam energy, and its quasi-melting and re-construction to form a polycrystalline junction at the soldered zone. It would be

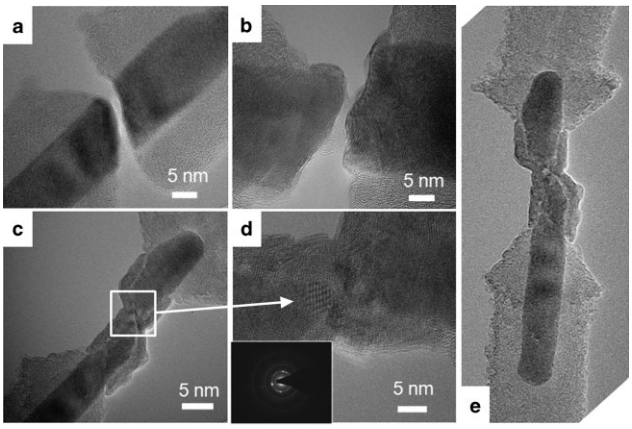

Figure 3. TEM images showing the nanosoldering of a cut Fe-filled MWCNT. a) Initial incision and gap-opening. b) Restructuring of the carbon walls surrounding the incision by e-beam irradiation (and initial exposure of the nanowire). c) Soldering back together of the Fe nanorods. d) High-resolution image of the soldered area. The inset shows a diffraction pattern recorded in the area. e) Low magnification image showing the completed soldering process.

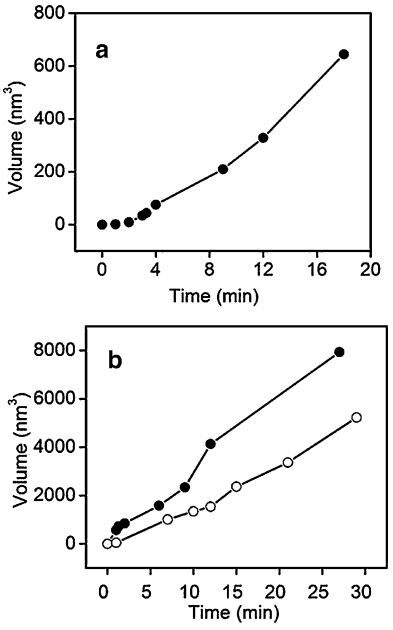

Figure 4. 'Growth' rate of the Fe nanorod outside of its original CNT enclosure expressed as exposed volume (nm^3) as a function of time (min) for: a) a 9 nm (inner)/32 nm (outer) diameter tube and b) for the nanosoldering process described in Figure 3.

interesting to study systematically the electrical properties of such junctions under variable irradiation conditions and different soldering materials. To further characterize the interconnection structure evolution, we recorded electron diffraction patterns (see inset of Fig. 3d) from the recrystallized area, after completing the tube's reconnection. We found scattered low intensity spots from polycrystalline iron and the presence of diffused rings typical of disordered carbon. A low magnification image of the final stage of the soldering process is shown in Figure 3e.

We analyzed the Fe nanorod 'growth' rate outside its original CNT enclosure in terms of volume of metal exposed as a function of irradiation time, on two independent samples that differ in inner and outer diameters (Fig. 4a and 4b). The plots show in all cases a rather nonlinear behavior, likely related to two leading phenomena: the sharpening/reshaping of the CNT's walls in the initial phase, followed by the forward movement, quasi-melting, and reconstruction of the metal tip. From these results it is clear that the amount of time necessary for nanosoldering depends on the geometry of the samples.

Through this work we present the first experimental demonstration of the use of nanoelectron beam engineering of MWCNTs as an advantageous tool for the creation of atomically sharp Fe-based tips. In addition, we report the creation of a CNT soldering iron and prove its effectiveness in the connection of two MWCNTs. The same approach can be used to solder a variety of different nanostructures. This system represents a viable tool for interconnecting nanowires, for example, in creating asymmetric heterostructures and heterojunctions.[17] Although far from being completely characterized, this work adds a new functionality in nanoelectromechanical systems and offers new avenues for further investigations.

Experimental

Growth of Fe-encapsulated MWCNTs: Fe-encapsulated nanotubes were grown by a chemical vapor deposition process using a two-stage thermal CVD system. The system consisted of a 30 mm diameter and 1000 mm long quartz tube that had a 200 mm preheating and 500 mm heating zone. The temperature controllers were set to desired temperatures (80 °C for the preheating zone and 825 °C for the heating zone). Si was used as a substrate for MWCNT growth. A mixture of Fe catalyst (ferrocene) and carbon source (toluene) (0.02 g mL^{-1}) were injected into the preheating zone at a rate of 0.3 mL min^{-1}. A flow of 100 sccm of argon gas was maintained as a carrier for the solution into the heating zone. The outer diameter of the grown CNTs ranged from 20–100 nm and their length was ~100 μm. For the TEM analysis, a small amount of deposited material was scratched from the substrate, dispersed in isopropyl alcohol and deposited on a perforated carbon-coated TEM grid.

Transmission Electron Microscopy: All experiments were carried out at room temperature in a TF 30 UT field-emission transmission electron microscope operated at 300 kV with no heating stage attached to the specimen holder. The field emission gun together with the probe forming lenses of the microscope are capable of producing a nanometer-sized electron beam with a current density of the order ~1.3×10^3 A cm^{-2}. Irradiation was carried out at beam current densities that varied from 1.3×10^3 to 7.5×10^2 A cm^{-2} on different diameter MWCNTs. Sequences of TEM images were recorded using a ORCA-ER camera with a 1280 × 1024 pixel format in a fixed bottom mount configuration and the camera used a Hamamatsu DCAM supported board for acquisition.

Acknowledgements

This work benefited from use of the Caltech KNI and Material Science TEM facilities supported by the MRSProgram of the National Science Foundation under Award Number DMR-0520565. The authors thank Prof. Florian Banhart for helpful discussions.

Received: July 5, 2008
Published online:

[1] M. Terrones, F. Banhart, N. Grobert, J.-C. Charlier, H. Terrones, P. M. Ajayan, *Phys Rev. Lett.* **2002**, *89*, 0 755 051.
[2] M. S. Wang, J. Y. Wang, Q. Chen, L.-M. Peng, *Adv. Funct. Mater.* **2005**, *15*, 1825.
[3] Y. Wu, P. Yang, *Adv. Mater.* **2001**, *13*, 520.
[4] P. W. Shutter, E. A. Shutter, *Nat. Mater.* **2007**, *6*, 363.
[5] C. Jin, Yung, K. Suenaga, S. Iijima, *Nat. Nanotechnol.* **2008**, *3*, 17.
[6] S. Heinze, M. Bode, A. Kubetzka, O. Pietzsch, X. Nie, S. Blugel, R. Wiesendanger, *Science* **2000**, *288*, 1805.
[7] Y. Saito, T. Yoshikava, M. Okuda, M. Ohkohchi, Y. Ando, A. Kasuya, Y. Nishina, *Chem. Phys. Lett.* **1993**, *209*, 72.
[8] Y. Saito, T. Yoshikava, M. Okuda, N. Fujimoto, S. Yamamuro, K. Wakoh, K. Sumiyama, K. Suzuki, A. Kasuya, Y. Nishina, *J. Appl. Phys.* **1994**, *75*, 134.
[9] J. X. Li, F. Banhart, *Nano Lett.* **2004**, *4*, 1143.
[10] F. Banhart, J. X. Li, M. Terrones, *Small* **2005**, *1*, 953.
[11] F. Banhart, *J. Mater. Sci.* **2006**, *41*, 4505.
[12] L. Sun, F. Banhart, A. V. Krasheninnikov, J. A. Rodriguez-Manzo, M. Terrones, P. M. Ajayan, *Science* **2006**, *312*, 1199.
[13] F. Banhart, J.-C. Charlier, P. M. Ajayan, *Phys. Rev. Lett.* **2000**, *84*, 686.
[14] F. Banhart, J. X. Li, A. V. Krasheninnikov, *Phys Rev. B* **2005**, *71*, 241 408.
[15] L. D. Marks, *Rep. Prog. Phys.* **1994**, *57*, 603.
[16] F. Banhart, *Rep. Progr. Phys.* **1999**, *62*, 1181.
[17] T. Mokari, C. G. Sztrum, A. Salant, E. Rabani, U. Banin, *Nat. Mater.* **2005**, *4*, 855.